
Universiteit
Leiden
The Netherlands

The maser strength of OH/IR stars, evolution of mass loss and the creation of a superwind

Baud, B.; Habing, H.J.

Citation
Baud, B., & Habing, H. J. (1983). The maser strength of OH/IR stars, evolution of mass loss and the creation of a superwind. *Astronomy And Astrophysics*, *127*, 73-83. Retrieved from https://hdl.handle.net/1887/6798

Version:	Not Applicable (or Unknown)
License:	Leiden University Non-exclusive license
Downloaded from:	https://hdl.handle.net/1887/6798

Note: To cite this publication please use the final published version (if applicable).

1983A&A...127...73B

Astron. Astrophys. 127, 73–83 (1983)

ASTRONOMY AND ASTROPHYSICS

The maser strength of OH/IR stars, evolution of mass loss and the creation of a superwind

B. Baud[1,2] and H. J. Habing[3]

[1] Kapteyn Astronomical Institute, Department of Space Research, P. O. Box 800, 9700 AV Groningen, The Netherlands
[2] Radio Astronomy Laboratory, University of California, Berkeley, CA 94720, USA
[3] Sterrewacht, P. O. Box 9513, 2300 RA Leiden, The Netherlands

Received November 25, 1982; accepted June 20, 1983

Summary. We study the statistical properties of OH/IR stars and attempt to relate these to current theories of stellar evolution on the Asymptotic Giant Branch (AGB) and the role therein of mass loss through a very dense stellar wind ("superwind"). First, we establish a quantitative relation between the OH luminosity L_{OH} and the mass loss rate $\dot{M}$. Second, we conclude that stars of the same main sequence mass can have very different values of $\dot{M}$, resulting in very different values of L_{OH} for the same value of the expansion velocity of the circumstellar shell, v_e. Since v_e is a measure of the main sequence mass M, this leads to the postulate that for a given M, $\dot{M}$ is increasing in time. The relative numbers of stars with different L_{OH} then imply an accelerated increase in mass loss rate. This is described by a slightly modified Reimers relation. In the emerging picture a star of given M, after reaching a certain point on the AGB (probably after the first thermal pulse), looses mass at a rapidly increasing rate until it has lost, in less than 10^6 yr, practically all of its envelope. This process occurs in such a short time that the total stellar luminosity, L_*, does not further increase. The picture is in agreement with the pulsational properties of OH/IR stars as a function of mass loss rate and leads to a relationship between L_* and v_e that is consistent with a stellar wind driven by radiation pressure on dust grains. Implications of these results in terms of stellar evolution, the effect of mass loss and the formation of planetary nebulae are discussed.

Key words: OH/IR stars – OH maser emission – mass loss – circumstellar shells – planetary nebulae – stellar evolution

1. Introduction

When a star begins to evolve away from the main sequence it also begins to lose mass, and this fact influences its further development. The rate at which mass is lost initially can be deduced from stellar parameters using the socalled Reimers relation (Reimers, 1975), and it ranges from 10^{-8} to $10^{-6}\,M_\odot\,\mathrm{yr}^{-1}$. Nevertheless, several observations indicate that considerably larger mass loss rates occur during short periods at the end of the evolution on the Asymptotic Giant Branch (AGB): (1) The discovery of infrared stars, i.e. thick spheres of gas and dust expanding from a late-type star, with mass loss rates much larger than the Reimers relation allows. The stellar radiation is completely converted into infrared radiation. Examples are IRC+10011, IRC+10216, and AFGL 2205. (2) The observed distribution of white dwarf masses (Weidemann, 1982; Koester and Weidemann, 1982) is rather narrow around a mean value of $0.58\,M_\odot$. If the evolution after the main-sequence lasted as long as is implied by the Reimers relation, than the core masses would grow beyond the range found for the white dwarfs: clearly more mass is ejected during the evolution. (3) Estimates of the mass, radius and expansion velocity of planetary nebulae give lower limits for the mass loss rate at the time of formation. These rates are a few times $10^{-5}\,M_\odot\,\mathrm{yr}^{-1}$. For stars approaching the end of the AGB (Iben and Renzini, 1982, preprint) this is at least an order of magnitude larger than deduced from the Reimers relation.

If stars lose most of their mass at the end of their evolution in a short, "superwind" phase (a term introduced by Renzini), then it is of great importance to study the statistical properties of the stars in this phase. Such stars must be infrared stars and statistical information is hardly existent, except for a subclass, called Type II OH/IR stars: evolved infrared stars at the top of the AGB (e.g. Wood, 1982), that are characterized by their double peaked OH maser emission which is strongest at 1612 MHz (Type II OH emission). They can be distinguished into two categories of objects: (1) optically known, long period variables and (2) IR point sources with no optical counterpart. The first category consists mainly of M type Mira variables of long periods ($P = 300$–500 d) with steeply rising light curves (Bowers and Kerr, 1977). Stellar luminosities are between 3000 and 15,000 $L_\odot$ and peak OH luminosities (defined as the peak OH flux at a distance of 1 kpc) are typically around 1–10 Jy kpc^2 (Nguyen-Q-Rieu et al., 1979). The expansion velocity of the gas/dust sphere, as deduced from the width of the OH line profile, can be between 5 and 25 km s^{-1}. Mass loss rates are estimated to be between 10^{-7} and $10^{-6}\,M_\odot\,\mathrm{yr}^{-1}$ (Hyland, 1974). We will call these objects "OH emitting Mira variables". In the second category we observe 1612 MHz OH emission from heavily obscured infrared stars, whose properties are in many ways similar to the Miras. They are usually found in unbiased radio surveys along the galactic plane. Whenever spectral information can be obtained, these OH/IR stars appear to be similar in spectral type to cool M giants (Jones et al., 1982a). The star is usually variable in the infrared with periods between 500 and 2000 d (Engels, 1982). The range in stellar luminosity is the same as for those in the first category but the OH luminosity is significantly larger: 50–1000 Jy kpc^2. Expansion velocities are in the range between 10 and 25 km s^{-1}; expansion velocities below 10 km s^{-1} are rarely found in the radio surveys. Mass loss rates are usually estimated between 10^{-5} and $10^{-4}\,M_\odot\,\mathrm{yr}^{-1}$ (Werner et al., 1980). In both categories there are

Send offprint requests to: B. Baud[1]

© European Southern Observatory • Provided by the NASA Astrophysics Data System

1983A&A...127...73B

indications that when the colors become redder the OH luminosity increases (e.g. Jones et al., 1982b).

Recent statistical studies at radio and infrared wavelengths have led to considerable advance in our understanding of the population and emission properties of these evolved stars. Three important conclusions form the basis of our study:

1. Baud et al. (1981, hereafter BHMW) have shown that the expansion velocity of the circumstellar shell, v_e (which is equal to half the velocity width ΔV between the two profile peaks), is correlated with age: the older the star, the smaller v_e. From the correlation between age and main sequence mass for stars in the solar neighbourhood BHMW deduced that OH/IR stars with $v_e = 10$–15 km s^{-1} have $M = 2$–$3\,M_\odot$ and for $v_e > 15$ km s^{-1}, $M > 3\,M_\odot$ and may be comparable to the OH emitting M supergiants found in the solar neighbourhood.

2. BHMW also found that the OH luminosity distribution $\psi(L_{OH})$ is broad, probably covering a range of a factor of 1000, and that the density of stars decreases steeply with increasing OH luminosity, L_{OH}. They showed that this is probably true for all values of $v_e > 10$ km s^{-1}, i.e. $\psi(L_{OH})$ appears to be independent of the main sequence mass for $M > 2\,M_\odot$, and they suggested that the same holds for the OH emitting Mira variables with $v_e < 10$ km s^{-1}. Also, Baud (1978) suggested that L_{OH} is *not* correlated with the stellar luminosity L_*. In the next section the observational evidence for this is summarized.

3. Engels (1982) shows that the infrared colours of OH/IR stars correlate with the period of light variation. A certain conclusion from their work is that thick circumstellar shells occur only for stars with extremely large periods ($> 1200^d$).

Is there a relation between the two categories of OH emitting late-type stars? Clearly, we would like to see them as two birds of the same feather, and several investigations have argued in favor of this. Originally, the apparent dichotomy between the OH luminosities was used to argue that the two groups are different, but we have shown elsewhere (BHMW) that a broad and steep OH luminosity distribution for all values of v_e, i.e. all main sequence masses, naturally explains this dichotomy as a result of observational selection. The basic parameter, that distinguishes the nearby, OH emitting Miras from the distant OH/IR stars appears to be the mass loss rate. The physical parameters that determine the OH luminosity are investigated in Sect. II and a relation is found between L_{OH} and the size of the circumstellar shell, which leads to a quantitative expression for L_{OH} as a function of the mass loss rate. By postulating in Sect. III that the OH luminosity function of OH/IR stars reflects the evolution in time of the OH luminosity for each star, we argue that the two categories are probably the two extremes of an evolutionary sequence in mass loss. Initially the stars are visible as OH emitting Mira variables and their mass loss rate is relatively low. Gradually their mass loss rate (and their OH luminosity) increases until they reach the obscured OH/IR phase. This postulate allows us to derive the evolutionary time-scale of mass loss from the observed distribution of OH luminosities: there are very few stars with large OH luminosity and thus high mass loss rates occur during a very short period, whereas the relatively large space density of stars with low OH luminosity indicates that the period of relatively low mass loss rate lasts much longer. The results are combined with the Reimers relation in Sect. IV to derive an expression for the evolution of mass loss in terms of the basic stellar parameters, which does incorporate the "superwind" phase. A new feature here is the dependence of the mass loss rate on the mass of the stellar envelope. The observed distribution of shell expansion velocities of OH/IR stars is then used in Sect. V to derive a quantitative relation between the expansion velocity and the main sequence mass of the star, which is in close agreement with the v_e-age relationship found by BHMW on kinematical grounds. This leads in Sect. VI to the derivation of stellar parameters based on the OH observations; the results are found to be consistent with independent information of stars at the tip of the AGB and with current ideas on stellar evolution in this part of the HR diagram.

2. OH luminosity and mass loss rate

What are the physical parameters that determine the OH luminosity of an OH/IR star? The correlated time variations of the OH and the infrared flux, and the modest amplitudes of the OH flux variations (Harvey et al., 1974) provide strong evidence that the 1612 MHz OH maser is radiatively pumped and that the maser is saturated. Elitzur et al. (1976) argue on theoretical grounds that (i) the pumping is done by 35 μm photons, produced by circumstellar dust reradiating the stellar light and (ii) L_{OH} is proportional to the 35 μm flux, L_{35}. Clearly, L_{35} itself will depend on the stellar luminosity L_*, but it will also depend on the efficiency by which the circumstellar shell transforms the stellar photons into 35 μm photons. This efficiency depends on the dust density in the shell and hence it must be a function of the mass loss rate.

For the unidentified OH/IR stars, L_* covers a range of only a factor of 30 from star to star ($2\,10^3$–$6\,10^4\,L_\odot$, see Jones et al., 1982b), while for the nearby Mira variables, which are among the least luminous OH masers, the stellar luminosity is typically of the same order, $10^4\,L_\odot$. Since L_{OH} can vary by more than three orders of magnitude between stars of the same main sequence mass, it is unlikely that L_* is a very important parameter in any quantitative expression for L_{OH}. The correlation between L_{OH} and the infrared colors suggest that the mass loss rate is probably an important factor in the OH luminosity. Since the mass loss rate is a function of the shell size (Bowers et al., 1981), we investigate below the relation between L_{OH} and the shell size.

For a number of OH/IR stars (Table 1, Column 1) the size of the circumstellar shell has recently been determined, either by intermediate resolution mapping of the extended low-brightness component of the OH emission (Booth et al., 1981; Bowers et al., 1981; Baud, 1981) or by measuring the phase delay between the light curves of the two profile peaks (Herman and Habing, 1981; Jewell et al., 1980). Column 2 gives the shell expansion velocity v_e, which is equal to half the velocity separation between the two OH emission peaks. In Column 3 the distance from the Sun is given, deduced from one of three different methods which are listed in the last column: (i) For some optically identified Mira variables we used the distances from Nguyen-Q-Rieu et al. (1979), based on a period-luminosity relation (P/L_*) for Mira variables. (ii) A few unidentified OH/IR stars near the galactic plane have very high radial velocities ($v_{lsr} > +100$ km s^{-1}) and are likely to be at the tangential point along the line of sight, nearest to the galactic centre, at a distance $D = R_\odot \sin l$, where $R_\odot$ is the distance of the galactic centre from the Sun (we have assumed $R_\odot = 10$ kpc) and l is galactic longitude. (iii) The distance to the other stars was determined geometrically (Schultz et al., 1978), using information on the angular size from the OH maps (Booth et al., 1981; Bowers et al., 1981; Baud, 1981) and the corresponding linear sizes from the OH phasedelay measurements of Herman and Habing (1981) and Herman (private communication). Bowers et al. (1981) list angular sizes based on maps of the integrated emission which is dominated by the peaks at the extreme ends of the line profile. Since the emission in the peaks originates from gas in a narrow double

© European Southern Observatory • Provided by the NASA Astrophysics Data System

1983A&A...127...73B

Table 1. OH/IR sources with measured shell sizes

Name	v_e km s^{-1}	Distance kpc	Radius 10^{16} cm	S_{OH} Jy	L_{OH} Jy kpc^2	$\dot{M}$ $10^{-5} M_\odot yr^{-1}$	
RS Vir	5	0.62	0.2*	2.5	1.0		P/L
IRC-20197	12	0.74	0.5	5.2	2.8	0.4[3]	1
RR Aql	6.5	1.1-0.6	0.8*	5.0	6.1-1.8		geom
U Ori	4	1.2	0.9*	3.5	5.0	0.12[2]	geom
IK Tau	17.5	0.27	1.2*	2.9	0.2	0.5[1]	1
VX Sgr	19.5	0.50	1.7	38.4	9.6		1
Z Cyg	2.5	0.8	2.0*	1.5	1.1		P/L
OH39.7+1.5	16.5	1.2-0.6	2.0*	44	63-16	2-5[3]	geom
R Aql	6.5	0.93-0.46	2.1*	14.2	12.3-3.0	0.08[2]	geom
WX Ser	7.5	4.1-2.1	2.4*	1.8	7.6-30.3	0.2-0.8[3]	geom
OH26.5+0.6	14.5	1.1	3.2*	206	250	2.6[5]	geom
OH25.1-0.3	12.5	9.1	3.5*	5.3	435	2.4[4]	tang
		3.4			61	0.9[4]	geom
IRC+10011	19	0.7	3.8*	23	11.3	1.7[1]	geom
OH17.7-2.0	12.5	2.9-1.4	4.7*	72	590-150		geom
OH127.8+0.0	11	3.3	5.3-10.6	27.9	304		kin
VY CMa	31.5	1.5	5.5	156	349	17-60[3]	
OH30.1-0.7	20.5	8.7	8.4*	44.8	3350	39[4]	tang
OH18.5+1.4	10.5	9.5	9.0*	5.4	484	0.4[4]	tang
OH32.8-0.3	16	6.1-3.1	11.7*	16.8	625-160	2-5[3]	geom

* determined from phase delay between the two emission peaks of the line profile (Herman and Habing 1981, Herman, private communcation)

(1) Hyland et al. (1972)

(2) Gehrz and Woolf (1971)

(3) Bowers et al. (1981)

(4) Baud, Werner and Bentley, in preparation

(5) Werner et al. (1980)

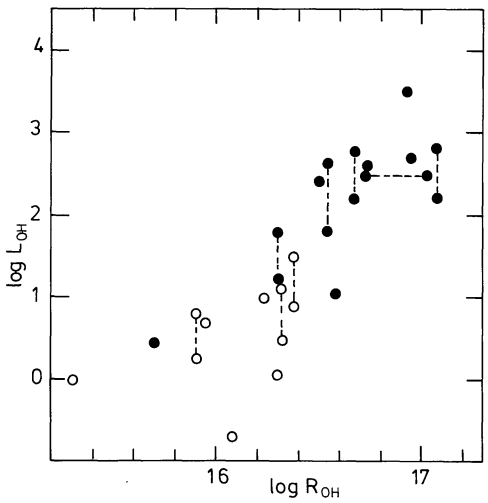

Fig. 1. L_{OH} (Jy kpc^2) as a function of the OH emitting shell radius (cm) of optically identified (○) and unidentified (●) OH/IR stars

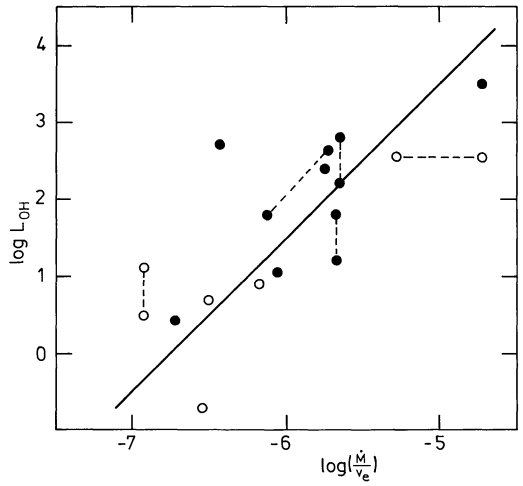

Fig. 2. OH luminosity as a function of mass loss rate ($M_\odot$ yr^{-1}) [see Eq. (4)] for those OH/IR stars, whose mass loss rate has been determined by infrared observations. v_e is deduced from the maser profile: $v_e = \Delta V/2$. The relationship predicted by Eq. (4) is also shown. Symbols are the same as in Fig. 1

cone along the line of sight through the star, the angular sizes thus derived are probably a lower limit and the corresponding geometrical distances are upper limits. Because the actual extent of the emission may be up to a factor of 2 larger (e.g. Baud, 1981), we have also given the parameters that correspond to half the distance upper limit. For IRC −20197 and VX Sgr the distance is based on a stellar luminosity of $10^4 L_\odot$ (Hyland et al., 1972) and for VY CMa on cluster association (Lada et al., 1978). Column 4 lists the linear radius of the OH emitting region, R_{OH}. An asterix denotes a size determination based on the phase-delay measurements between the two peaks of the line profile. This is a direct measure of the size of the shell along the line of sight, and is *independent* of the assumed distance. In the other cases the linear sizes are derived from the angular sizes of the OH maps and they are therefore distance dependent. Uncertainty in R_{OH} is about a factor of 2. Column 5 lists the mean OH peak flux density S_{OH}, taken from the literature and in some cases from recent measurements with the Dwingeloo 25 m telescope (Herman, private communication). Following BHMW, S_{OH} is defined as the geometric mean of the peak flux of the two emission components S_1, S_2, ($S_{OH} = (S_1 S_2)^{1/2}$), corrected to a resolution of 6.5 kHz in a manner described by Baud et al. (1979). When variability information was available we have taken the peak flux averaged over the lightcurve. Column 6 contains the corresponding OH luminosity $L_{OH} = S_{OH} D^2$, where D is the distance in kpc. The mass loss rates in Column 7 are based on infrared observations, in some cases corrected for the distances used in this paper.

In Fig. 1 L_{OH} is plotted as a function of R_{OH}. In spite of the scatter and the uncertainty in both L_{OH} and R_{OH}, there is a clear trend of a steeply increasing OH luminosity with increasing shell radius, both for the visible and the unidentified OH/IR stars. The overlap in both L_{OH} and R_{OH} confirms the continuous transition in circumstellar and OH properties between nearby, visible OH emitting Miras and M supergiants, and their unidentified counterparts found in surveys at large distances from the Sun, also noted by Nguyen-Q-Rieu et al. (1979).

The data in Fig. 1 suggest that L_{OH} is proportional to R_{OH}^p, where p is the slope in the data points. An eyeball estimate suggests a slope between 2 and 3. For reasons, listed below, we prefer the lower value, $p = 2$.

© European Southern Observatory • Provided by the NASA Astrophysics Data System

1983A&A...127...73B

(1) We have assumed $R_\odot = 10$ kpc. For a smaller value, three points in Fig. 1 (OH 25.1 −0.3, OH 30.1 −0.7, OH 18.5 +1.4) in the upper right will shift downward.

(2) A slope of 2 gives a better fit to the independent mass loss determinations, based on infrared observations (see below and Fig. 2), and it is also confirmed by more recent work (Herman, thesis Leiden 1983).

A linear fit using a slope of 2 yields the following relationship

$$L_{OH} = 4(\pm 2) R_{OH}^2 \text{ Jy kpc}^2. \quad (1)$$

R_{OH} is in units of 10^{16} cm[1].

Equation (1) now allows us to derive a more physical relation between L_{OH} and $\dot{M}$. For a steady flow the mass loss rate is given by

$$\dot{M} = 4\pi \varrho(R_{OH}) v_e R_{OH}^2, \quad (2)$$

where $\varrho(R_{OH}) = n_{H_2}(R_{OH}) \times \mu(H_2)$ is the mass density of the shell at distance R_{OH} from the star. We assume that R_{OH}, the radius at which the OH maser occurs, is rather sharply defined. Aperture synthesis observations confirm this (Booth et al., 1981; Baud, 1981). The pump model of Elitzur et al. (1976) indicates that saturation of the 1612 MHz OH maser requires a minimum OH column density of about 10^{17} cm^{-2}, corresponding to a molecular hydrogen column density of (Goldreich and Scoville, 1976)

$$N(H_2) = 6\ 10^{20} \text{ cm}^{-2}. \quad (3)$$

Because the surface brightness of the OH maser emission appears to be approximately constant [cf. Eq. (1)], we will assume that Eq. (3) holds for all saturated masers. Using Eq. (2) it can be shown easily that the density integrated outward from R_{OH} equals $N(H_2) = n_{H_2}(R_{OH}) \times R_{OH}$. Substituting R_{OH} in Eqs. (1) and (2), and using Eq. (3) we find that

$$L_{OH} = 3\ 10^{13} \left(\frac{\dot{M}}{v_e}\right)^2 \text{ Jy kpc}^2. \quad (4)$$

$\dot{M}$ in $M_\odot$ yr^{-1} and v_e in km s^{-1}. The normalisation constant is uncertain by at least a factor of 2.

Equation can be checked using independently determined mass-loss rates. Infrared observations yield typical values of $5\ 10^{-6} M_\odot$ yr^{-1} for the visible OH/IR stars (Hyland, 1974) and about $3\ 10^{-5} M_\odot$ yr^{-1} for the unidentified stars (Werner et al., 1980). The predicted OH luminosities for $v_e = 15$ km s^{-1} of 4 and 130 Jy kpc^2 respectively are in good agreement with the typical OH luminosity observed for these objects, suggesting that Eq. (4) is qualitatively consistent with independent infrared and radio observations. This conclusion is further strengthened in Fig. 2 by considering the OH luminosities of those stars in Table 1 whose mass-loss rates have been determined independently by infrared observations. Although the uncertainties in these mass loss rates are large, most points lie near the line defined by Eq. (4), indicating that the predicted steep increase in L_{OH} with $\dot{M}$, deduced from the OH observations, is indeed consistent with the infrared observations. Hence Eq. (4) adequately describes the transition of circumstellar and OH properties between the weak, nearby OH emitting Miras and the very bright and distant, unidentified OH/IR stars as a transition to higher mass loss rates. Moreover, the large range in L_{OH} seen in OH/IR stars corresponds to a relatively small range in $\dot{M}$.

Several authors have previously argued for a relation between L_{OH} and $\dot{M}$. For example, Nguyen-Q-Rieu et al. (1979) show a diagram in which L_{OH} correlates with the [3.5 μm]–[10 μm] colour of the star. Similarly, Jones et al. (1982b) show a convincing correlation between L_{OH}/L_* (in their terms: $M_{bol} - M_{OH}$) and the infrared colour L–M. In an ongoing program of infrared observations our collaborators and we find a tight correlation between the [4.8 μm]–[12.5 μm] colour and L_{OH}/L_{IR}. However, as far as we know, an explicit and quantitative relation between L_{OH} and $\dot{M}$, as in Eq. (4), has not yet been published.

3. OH luminosity distribution and the evolution of mass loss

In Sect. II we found that the OH luminosity is determined primarily by the mass loss rate. The observations show that L_{OH} is proportional to $\dot{M}^2$. Since the OH luminosity distribution is broad and, to first order, independent of main sequence mass (see Sect. I), we conclude that OH/IR stars of a given main sequence mass can be found on the AGB with widely different values of L_{OH}, i.e. with quite different mass loss rates. This conclusion suggests that for a star of a given mass the OH luminosity, and consequently the mass loss rate, is a function of time and that *the steep* OH *luminosity function reflects the increase of* L_{OH} *and of the mass loss rate of each star as it moves up the* AGB. When a star enters the AGB its mass loss rate will initially be too low for a 1612 MHz OH maser to operate. As the star evolves its mass loss rate increases. At some point the maser will turn on and it will increase in strength with increasing $\dot{M}$. In this picture stars with the highest L_{OH} must be in the final, superwind phase of their AGB evolution and their mass loss rate suggests that they must soon be entering the PN stage. The fact that there are fewer stars with high and more with low OH luminosity, implies that the high luminosity (high mass loss rate) phase is much shorter than that of low OH luminosity (small mass loss rate). In other words, the steep shape of the OH luminosity function reflects a rapid acceleration of mass loss rate as the star evolves through the superwind phase.

In a previous paper (BHMW), we have introduced the OH luminosity function $\psi(L_{OH}) dL_{OH}$ as the number of OH/IR stars with OH luminosity between L_{OH} and $L_{OH} + dL_{OH}$. There we concluded that $\psi \varrho L_{OH}^{-\alpha}$ with $\alpha = 1.65$. Olnon (private communication) has reanalyzed three 1612 MHz OH surveys and he concludes that each survey yields $\alpha = 2 \pm 0.1$. We shall use Olnon's more accurate value because it applies to a larger data set with a lower sensitivity limit than BHMW's sample and it is derived by making a more careful analysis of the various observational selection effects.

With this expression for the OH luminosity distribution the evolution of the OH luminosity in time can now be derived. If N_{OH} is the total number of OH/IR stars, integrated over all values of L_{OH}, and t_{OH} is the duration of the OH emitting phase, then

$$\psi(L_{OH}) dL_{OH} = \beta L_{OH}^{-\alpha} dL_{OH} = \frac{L_{OH}}{t_{OH}} dt,$$

where $\alpha = 2$ and β is the normalization constant of $\psi(L_{OH})$. We assume that at $t = 0$ the mass loss rate is at the minimum value required to turn the 1612 MHz OH maser on at the initial OH luminosity L_{min}. At the end of the AGB evolution, when $t = t_{OH}$, the OH luminosity will reach a maximum value L_{max}. With these

1 More recent determinations of the phase delay by Herman (1983, PhD thesis Leiden), based on the emission at all velocities between the peaks, show for some stars somewhat smaller radii than listed below, resulting in a correspondingly smaller distance. However, this does not affect our results in Fig. 1 since this represents only a small shift parallel to the trend in the data

© European Southern Observatory • Provided by the NASA Astrophysics Data System

1983A&A...127...73B

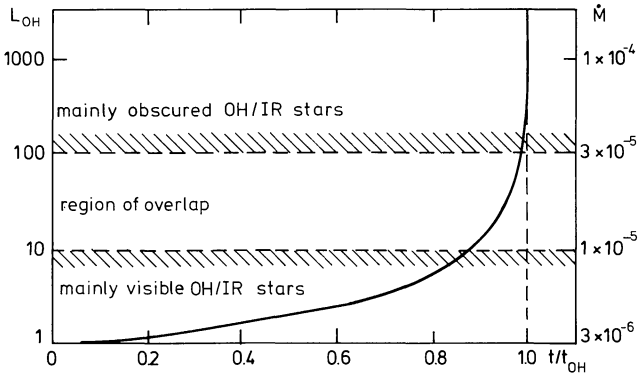

Fig. 3. OH luminosity and mass loss rate as a function of time [Eqs. (5) and (6)] in units of the OH maser lifetime t_{OH}. t_{OH} ranges from 0.6 to 6 10^5 yr for main sequence masses from 0.7 to 6 $M_\odot$ (see Table 2). Most of the time is spent at low mass loss rate, when the star remains visible. Only during the last 1 % of its OH lifetime is a star bright enough to be seen throughout the Galaxy as an OH/IR star. This is probably the superwind phase, which lasts for 10^2–10^3 yr. The evolution of mass loss is expressed in the "Modified Reimers Relation" [Eq. (10)]

Table 2. Stellar parameters of OH/IR stars

v_e kms^{-1}	M $M_\odot$	$\dot{M}_0$ $10^{-6}M_\odot yr^{-1}$	$M_{co,0}$ $M_\odot$	$M_{co,tp}$ $M_\odot$	KWII $M_\odot$	$L_{*,0}$ $10^4 L_\odot$	$M_{e,0}$ $M_\odot$	t_{OH} 10^5 yr	N	L_{max} Jykpc^2	N'
(1)	(2)	(3)	(4)	(5)	(6)	(7)	(8)	(9)	(10)	(11)	(12)
6	0.7	1.1	0.59	0.53	0.60	0.5	0.11	0.6	128	37	0
9	1.0	1.5	0.64	0.54	0.63	0.8	0.36	1.4	116	82	0
11	1.5	2.0	0.71	0.56	0.68	1.2	0.79	2.0	73	112	13
14	2.1	2.4	0.80	0.61	0.75	1.8	1.30	2.8	42	175	29
16	3.1	2.9	0.93	0.72	0.85	2.5	2.17	3.7	23	236	21
19	4.4	3.3	1.10	0.88	0.99	3.5	3.30	5.0	12	318	14
21	6.3	3.8	1.34	0.97	1.19	5.0	4.96	6.5	6	411	7
24	9.0	4.2	>1.4	-	>1.4	-	-	0	0	-	0

Explanation (see also text). v_e: expansion velocity of the circumstellar shell. M: main sequence mass of the star. $\dot{M}_0$: mass loss rate when the 1612 MHz OH maser turns on (t=0). $M_{co,0}$: core mass at t=0. $M_{co,tp}$: core mass when the first thermal pulse occurs (Iben 1981). KWII: mass of white dwarf resulting from the main sequence mass in col. 2, according to Koester and Weidemann (1980). $L_{*,0}$: bolometric luminosity of the star at t=0. $M_{e,0}$: envelope mass at t=0. t_{OH}: stellar lifetime after the maser has turned on. N: relative space density (arbitrary units) of OH/IR stars with an OH luminosity larger than BHMW's survey sensitivity limit L_s = 100 Jy kpc^2 and not corrected for maser turn off in the final stage. L_{max}: maximum OH luminosity to be reached. N': relative space density of OH/IR stars with $L_{max} > L_{OH} > L_s$

boundary conditions the expression for β is

$$\beta=\frac{N_{OH}(1-\alpha)}{L_{max}^{1-\alpha}-L_{min}^{1-\alpha}}.$$

From Table 1 we deduce reasonable values for L_{min} and L_{max} of 1 and 1000 Jy kpc^2 respectively. The evolution of L_{OH} in time is then given by

$$L_{OH}(t)=L_{min}\left[1-A\frac{t}{t_{OH}}\right]^{\frac{1}{1-\alpha}}, \quad (5)$$

where $A=1-(L_{max}/L_{min})^{(1-\alpha)}$. Using Eqs. (4) and (5), and assuming that v_e is constant in time for a given OH/IR star, the evolution of mass loss rate in the final stages of AGB evolution is then

$$\dot{M}(t)=\dot{M}_{min}\left[1-B\frac{t}{t_{OH}}\right]^{\frac{1}{2(1-\alpha)}} \quad (6)$$

where $B=1-(\dot{M}_{max}/\dot{M}_{min})^{2(1-\alpha)}$. $\dot{M}_{min}$ and $\dot{M}_{max}$ are the mass loss rates corresponding to L_{min} and L_{max} at times $t=0$ and t_{OH}. The assumption of constant v_e is unavoidable: significant change in v_e during the evolution on the AGB would be inconsistent with the observed correlation between v_e and stellar age (and thus M) found by BHMW.

We may take A and B equal to 1 for the large range observed in L_{OH} and $\dot{M}$. Strictly speaking this means [see Eqs. (5) and (6)] that when $t\to t_{OH}$, then $\dot{M}\to\infty$ and $L_{OH}\to\infty$. However, this is a problem only during the very last pulsations, and some other process will suppress the singularity (see Sect. V). L_{min}, L_{max}, $\dot{M}_{min}$, $\dot{M}_{max}$, and t_{OH} may not be the same for all stars; in fact we will show later that L_{max}, $\dot{M}_{max}$, and t_{OH} are a function of the main sequence mass.

A graphical representation of Eqs. (5) and (6) with $\alpha=2$, $L_{max}=1000$, and $L_{min}=1$ Jy kpc^2 is shown in Fig. 3. It is clear that most of the time the OH emission is very weak and close to L_{min}. This is the stage of the OH emitting Miras in the solar neighbourhood. Only in the final stages of its AGB evolution is an OH/IR star bright enough to be detected throughout the Galaxy. We propose that this is the phase of the "superwind". Although the transition between the two mass loss phases in our model is smooth, we cannot exclude the possibility of a discontinuity between the Mira mass loss phase and the superwind phase, as is favored by Renzini (1981). Our result is a natural consequence of the smooth OH luminosity function used by BHMW, but we should note that BHMW's data were insufficient to exclude a bimodal luminosity function that would exist if the transition from wind to superwind were very abrupt. However, our result of a very rapid increase of $\dot{M}$ near the end of the OH phase (cf. Fig. 3) does not differ very much from such a discontinuous transition in mass loss rate.

What is the duration of this very bright OH maser phase? The time spent by a star with L_{OH} larger than a given value L_c is $\Delta t=t_{OH}-t_c$, with t_c the time needed to reach L_c. It follows from Eq. (5) that $\Delta t=t_{OH}(L_{min}/L_c)$. We then find that the distant, unidentified OH/IR stars, which have a typical OH luminosity $L_c\geqq100$ Jy kpc^2, are in the last 1 % of their lifetime as an OH emitter. This estimate is confirmed when considering the observed number of weak and very luminous OH/IR stars within one kpc from the Sun. From radio surveys of nearby Miras, M supergiants and IRC sources we find about 45 with Type II OH emission, most of which are relatively weak ($\ll100$ Jy kpc^2), except for the supergiant NML Cyg. This number is probably an underestimate because all OH surveys are flux limited and are therefore incomplete at the low end of the luminosity distribution. Unbiased radio surveys along the plane have revealed only one more luminous nearby OH/IR star, OH 26.5+0.6. This means that less than 4 % of the OH/IR stars in the solar neighbourhood are of the luminous kind, consistent with the prediction of about 1 %.

If the total mass lost during the OH lifetime is equal to the initial envelope mass of the star (see Sect. IV), t_{OH} can be calculated by integrating Eq. (6) from $t=0$ to $t=t_{OH}$,

$$t_{OH}=\frac{M_{e,0}}{2\dot{M}_{min}}, \quad (7)$$

© European Southern Observatory • Provided by the NASA Astrophysics Data System

1983A&A...127...73B

where $M_{e,0} = M - M_{co,0}$ is the initial envelope mass and $M_{co,0}$ is the core mass at the beginning of the OH maser phase at $t = 0$ (subscript 0). With a typical OH lifetime of 10^5 yr (see Sect. V, Table 2), the lifetime of the superwind is about 10^3 yr, depending on the main sequence mass of the star.

4. Evolution of mass loss in terms of stellar parameters

In current research on the evolution of stars on the Giant Branch and on the Asymptotic Giant Branch one often uses the mass loss rate as given by the so called Reimers relation (Reimers, 1975)

$$\dot{M} = -4\ 10^{-13}\eta \frac{L_* R_*}{M}\ M_\odot\ \mathrm{yr}^{-1}, \tag{8}$$

where L_*, R_*, and M are in solar units. The constant η is of order unity (Renzini, 1981). Reimers' relation was established empirically from optical observations and a solid theoretical explanation has not yet been found. It has the disadvantage that it is not applicable to the OH or superwind phase discussed here, because the predicted mass loss rates are too small. Nevertheless, an attractive feature of the Reimers relation is its dependence on stellar parameters, which can in principle be determined observationally. Here we show that Eq. (6), which does indeed predict a much steeper increase in the mass loss rate at the end of the AGB evolution, also leads to an expression for the evolution of mass loss in terms of stellar parameters, which may be physically more meaningful than the Reimers relation.

Taking $B = 1$ and $\alpha = 2$ in Eq. (6) and using Eq. (7) it follows that the total amount of matter lost from the star up to time t is

$$M_{\mathrm{lost}}(t) = M_{e,0}\left[1 - \left(1 - \frac{t}{t_{\mathrm{OH}}}\right)^{1/2}\right].$$

Substituting the rest envelope mass at time t, $M_e(t) = M_{e,0} - M_{\mathrm{lost}}(t)$ we find that $M_e(t)/M_{e,0} = (1 - t/t_{\mathrm{OH}})^{0.5}$ and Eq. (6) transforms to

$$\dot{M}(t) = \frac{\dot{M}_{\min} M_{e,0}}{M_e(t)}. \tag{9}$$

Assuming that at $t = 0$ the stellar mass is equal to the main sequence mass M, then $\dot{M}_{\min}$ is given by the Reimers relation (8). Hence we derive a mass loss rate

$$\dot{M}(t) = \mu \frac{L_* R_*}{M_e(t)} \tag{10}$$

with $\mu = -4\ 10^{-13}(M_{e,0}/M)$. The fundamental difference between the Reimers relation and our Eq. (10) (which we will call the modified Reimers relation) is the dependence on M_e instead of M. During most of the AGB evolution, when the mass loss rate is relatively low, M_e is nearly equal to M for $M > 2\,M_\odot$, implying that both the Reimers relation and our modified version are approximately equal. At the end of the AGB evolution the reduced envelope mass forces the mass loss rate to increase steeply, reaching much higher values than predicted by the standard Reimers relation. We propose that our Eq. (10) is in fact a better representation of the mass loss rate over the whole AGB evolution than the Reimers relation.

The validity of various assumptions, implicit in the discussion, are considered below.

1. We have assumed that at the beginning of the OH maser phase ($t = 0$) the stellar mass is equal to the main-sequence mass. According to Iben (1981) Cepheids, which are in the core-helium burning phase just before reaching the AGB, have a pulsational mass that is still within 20 % equal to their main-sequence mass as deduced from stellar evolution theory. This suggests that little mass has been lost between the main-sequence and the initial AGB phase. Furthermore, as the star enters the AGB, mass will be lost initially at a relatively low rate as expressed by the standard Reimers relation. With a total AGB time of (1–2) 10^6 yr (Renzini, 1981) and an average Reimers mass loss rate of 10^{-7}–$10^{-6}\,M_\odot\ \mathrm{yr}^{-1}$, the amount of mass lost during the AGB before the OH maser phase will also be a fairly small fraction of the initial envelope mass. Hence, it is reasonable to assume that the mass of an OH/IR star at the onset of the superwind is approximately equal to its main-sequence mass.

2. During the OH maser phase the stellar luminosity and radius are assumed to be constant. The stellar luminosity in these final stages is ony a function of the core mass (Paczyński, 1970),

$$L_* = 5.9\ 10^4 (M_{co} - 0.5)\, L_\odot, \tag{11}$$

where M_{co} is in units of $M_\odot$. Due to nuclear burning in the H- and He-burning shells the core mass grows exponentially until the Chandrasekhar limit of $1.4\,M_\odot$. Using the core growth rate given by Iben (1981) and an AGB lifetime of 10^6 yr, we find that L_* will increase by not more than 60 % during that time. Since the effective temperature is roughly constant during most of the AGB evolution, the change in R_* during that time must be small, probably less than a factor of two. In practice the product $L_* R_*$ will probably increase by at most a factor of two. This is much smaller than the rapid increase of $\dot{M}$ by at least an order of magnitude during the OH maser phase. Hence, our assumption of constant L_* and R_* seems justified.

3. For simplicity in the calculations it has been assumed that at the end of the superwind phase, at $t = t_{\mathrm{OH}}$, the whole envelope is shed and only the core remains. Renzini (1981) argues that at the end of the AGB evolution, when the star slowly evolves to the left of the AGB, the superwind terminates before the final ejection of the envelope and that the mass loss rate will slow down to a normal Reimers wind when $M_e = 0.005$–$0.01\,M_\odot$. This implies that the superwind will actually terminate 50–100 yr sooner, which is less than 0.1 % of the total OH lifetime. This premature termination of the superwind therefore does not affect the total evolution of the OH/IR star, except that it suppresses the divergence of $\dot{M}$ when $t = t_{\mathrm{OH}}$ (see Sect. V).

5. The relation between main sequence mass and expansion velocity

The discussion so far shows that the mass loss rate of OH/IR stars can be derived from the OH luminosity and that the evolution of mass loss rate at the end of the AGB, as deduced from *circumstellar* parameters [Eqs. (6) and (10)], is a natural extension of the Reimers mass loss, which can be expressed in terms of *stellar* parameters. By using the OH data on the circumstellar shells it may therefore be possible to derive information on the star itself and its evolution on the AGB. A first indication of this interesting possibility is the statistical correlation between v_e and stellar age, i.e. main sequence mass, found by BHMW. The results in the previous sections now allow us to derive a more quantitative relation between v_e and the main sequence mass M which takes into account the results of BHMW. In Fig. 4a we show the distribution of shell expansion velocities of a sample of nearby OH/IR stars which mainly consists of optically identified Miras or supergiants

© European Southern Observatory • Provided by the NASA Astrophysics Data System

1983A&A...127...73B

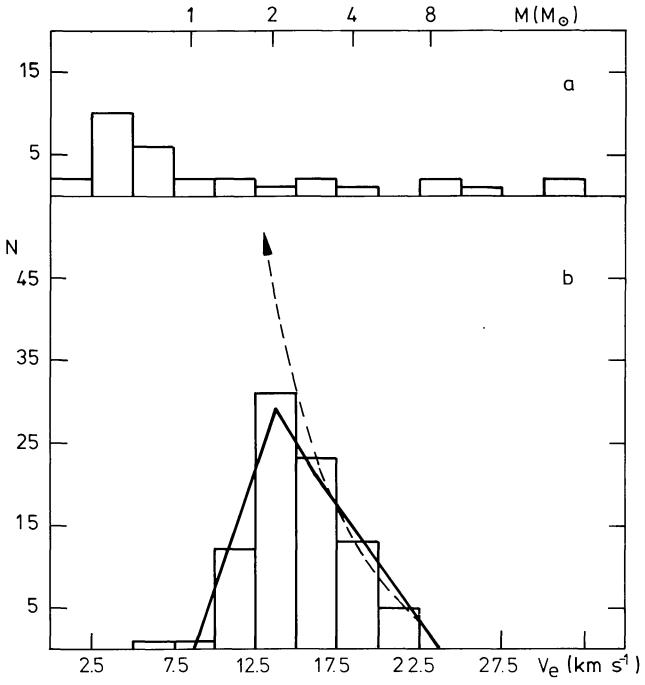

Fig. 4a and b. Histogram of v_e values for **a** the nearby, optically identified Miras and M supergiants that are strongest at 1612 MHz (Type II OH/IR) and **b** unidentified OH/IR stars from BHMW, found between $l=10°$ and 50°. The two curves represent the model fits described in Sect. V. Dashed line is the theoretical distribution without a cut-off in L_{OH}; full drawn line is the theoretical distribution with a cut-off $L_{max}(v_e)$ [see Eq. (14)]

with intrinsically weak Type II OH emission. They are taken from the OH surveys of nearby Miras (<1 kpc) by several authors (Nguyen-Q-Rieu et al., 1979; Olnon et al., 1979; Engels, 1979; and Wilson and Barrett, 1972). Figure 4b contains the distant, unidentified OH/IR stars with high OH luminosity, found in radio surveys throughout the Galaxy and taken from the homogeneous sample of BHMW in the longitude interval $l=10°$–50°. Most of these are in the molecular ring at a distance of 7–10 kpc from the Sun. The difference between the distributions is striking. The OH emitting Mira variables have a very broad distribution, ranging from 3 to 30 km s^{-1}, with a weak maximum at the lowest values of v_e. The unidentified OH/IR stars appear to have a much narrower distribution with a pronounced maximum around 15 km s^{-1} and there is an obvious lack of stars below 10 km s^{-1}, where most of the optically identified stars occur. Although the optically identified sample is not very homogeneous, this difference cannot be due to observational selection effects alone and must be real. The implication is that only very few stars with $v_e<10$ km s^{-1} and main sequence masses below about $2\,M_\odot$ (BHMW) reach very high values of L_{OH}. This is contrary to the suggestion of BHMW that, to first order, $\psi(L_{OH})$ is independent of v_e.

We will use the homogeneous and well defined sample of OH/IR stars of BHMW to derive an expression for the v_e-distribution by comparing the observations compiled in Fig. 4b with the distribution function of stellar masses. Bowers (1978) and BHMW found that most OH/IR stars are located in the molecular ring at $R=5$ kpc and at approximately the same distance from the Sun. Consequently, we may assume that the sample in Fig. 4b consists of all OH/IR stars above a certain minimum OH luminosity L_s, which corresponds to BHMW's survey sensitivity limit. Since v_e and M are correlated, the observed v_e-distribution, $N(v_e)\,dv_e$, is equivalent to the number density of OH/IR stars with mass M per dM-interval with $L_{OH}>L_s$, $N(M, L_s)\,dM$. The quantity $N(M, L_s)$ is proportional to the total number density of stars with mass M, the fraction of the total stellar lifetime that a star of mass M spends as an OH/IR star, and the fraction of OH/IR stars of mass M with $L_{OH}>L_s$:

$$N(M,L_s)\,dM=\varphi(M)\,\frac{t_{OH}}{t_*(M)}\left[\int_{L_s}^{\infty}\frac{\psi(L_{OH})}{N_{OH}}\,dL_{OH}\right]dM,$$

where φ(M) is the present-day-mass-function, t_{OH} is the total OH maser lifetime, $t_*(M)$ is the main-sequence lifetime of a star with mass M, and N_{OH} is the OH/IR star density, integrated over all OH luminosities. Following BHMW, we assume for the moment that $\psi(L_{OH})$ is independent of v_e or main sequence mass of the stars. Later in this section we will return to the contradiction noted above. Furthermore, the fraction of stars that become OH/IR sources in the course of their evolution towards the top of the AGB is assumed to be independent of v_e (mass). For the masses considered here ($>1\,M_\odot$), the ratio $\varphi(M)/t_*(M)$ is equal to the initial mass function $\xi(M)$. Miller and Scalo (1979) find that $\xi(M)\propto M^{-2.5}$ for $M=1$–$10\,M_\odot$. With $\psi(L_{OH})$ given as in Sect. III it follows that

$$N(M,L_s)\,dM=CM^{-2.5}\,t_{OH}M)\,\Lambda(L_s), \tag{12}$$

where $\Lambda(L_s)=(L_{max}^{-1}-L_s^{-1})/(L_{max}^{-1}-L_{min}^{-1})$. C is a normalization constant that includes the absolute calibration of the IMF and the OH luminosity function. Since t_{OH} is a slowly increasing function of the main sequence mass (see below), it is clear from Eq. (12) that the number density of OH/IR stars must steeply decrease with increasing mass and therefore with increasing v_e, as is the case for $v_e>15$ km s^{-1}. This part of the v_e-distribution is simply a reflection of the steep initial mass function and it allows us to determine more precisely the functional relationship between v_e and M. A first estimate of the shape of this relationship can be obtained from our knowledge of the population characteristics of OH/IR stars and optically identified Miras. Stars with $3<v_e<10$ km s^{-1} are mainly Miras with periods ranging from 300 to 500 d and a main sequence mass of about $1\,M_\odot$. BHMW found that for $10<v_e<15$ km s^{-1} the kinematics of the stars were consistent with a mass of 2–3 $M_\odot$ and that for $v_e>15$ km s^{-1} most stars must be similar to the M supergiants, with $M>3\,M_\odot$ and possibly ranging up to $10\,M_\odot$. This suggests an increasingly steeper relation between v_e and M with increasing values of v_e. We have taken the following expression

$$v_e=\gamma\,\log\left(\frac{M}{M_\odot}\right)+\delta\ \text{km s}^{-1}. \tag{13}$$

Using the various relations deduced in this paper we are now able to derive stellar properties of OH/IR stars at the beginning of the OH maser phase, their OH lifetime and relative number density for a range of main sequence masses, with γ and δ as free parameters. These can be determined subsequently by fitting Eq. (12) iteratively to the observed v_e-distribution in Fig. 4b, using L_{max} and L_{min} of 1000 and 1 Jy kpc^2 and for a given value of L_s. For BHMW's sample $L_s=100\pm20$ Jy kpc^2. The procedure is described in the appendix. After two iterations we obtained an optimum fit to the observed distribution in Fig. 4b with the following values: $\gamma=16\pm1$ and $\delta=8\pm2$ km s^{-1}.

© European Southern Observatory • Provided by the NASA Astrophysics Data System

1983A&A...127...73B

The calculated density distribution $N(M, L_s)$, using these values for γ and δ, is listed in Table 2, column 10, and shown in Fig. 4b (dashed). It is clear that this simple model predicts the observations reasonably well at the high mass end of the distribution. The numbers below $v_e = 15$ km s^{-1} are severely overestimated, but the resulting mass scale (top of Fig. 4) is nevertheless in good agreement with the first order estimate of BHMW's approximate relation between main sequence mass and v_e, based on the kinematics of OH/IR stars. This gives us confidence that our approach is correct and the assumptions are reasonable. Note also that the distribution of stars with low L_{OH} (Fig. 4a) qualitatively agrees with these model calculations, with the numbers increasing with decreasing v_e (mass). However, only very few stars with $v_e < 15$ km s^{-1} appear to evolve to high values of L_{OH}, i.e. high $\dot{M}$, as is clear from Fig. 4b.

What is the reason for the apparent lack of low mass OH/IR stars with high OH luminosity and correspondingly high mass loss rates? We propose two possible explanations which might be valid separately and simultaneously.

(1) As the star evolves, the expansion time of the circumstellar shell will increase with time, since the OH emitting radius moves slowly outward with increasing $\dot{M}$. Simultaneously, the mass is lost at a growing rate – see Eq. (6). Initially, the evolution of mass loss rate is slow (Fig. 3) and the maser radius is small, so that ejection of the gas from the star out to the maser radius is instantaneous. But in the final stages of the evolution on the AGB, when the mass loss rate is very high, the time that is left to eject the rest envelope, Δt, will become comparable to the expansion timescale of the circumstellar shell. The assumption of instantaneous ejection is no longer correct. When the envelope has been ejected completely, leaving only a hot stellar core, the inner shell will be heated up and ionized in a very short time (10^3 yr). Before the matter ejected last has reached the OH maser region, the number of pump photons will decrease dramatically, limiting the maximum OH luminosity that the star will reach. This maximum luminosity L_{max} will occur (see Sect. III) at a time $\Delta t = t_{OH}(L_{min}/L_{max})$ before the end of the OH phase. Equating Δt to the expansion timescale $t_{exp} = R_{max}/v_e$, where $R_{max} = (L_{max}/4.2)^{0.5}$ [from Eq. (1)] it is found that

$$L_{max} = 2.8\ 10^{-3}\ (t_{OH} L_{min} v_e)^{2/3}. \quad (14)$$

It is clear from Eq. (14) that the maximum OH luminosity increases with increasing v_e. Column 11 in Table 2 lists these maximum values L_{max}. For a typical minimum detectable luminosity at a distance of 5 kpc of about 100 Jy kpc^2 for the sample of OH/IR stars (BHMW), we expect to find no stars with $v_e < 10$ km s^{-1}, since their maximum luminosity lies below the survey sensitivity limit. The fact that BHMW's sample contains some stars with $v_e < 10$ km s^{-1}, that have values of L_{OH} well above 100 Jy kpc^2, suggests that a small percentage of stars overshoot their maximum OH luminosity. This could be due to the extreme sensitivity of the detailed evolution of the superwind to the initial conditions, such as the phase of pulsation at the onset and the termination of the superwind (Iben and Renzini, 1982).

(2) Another possibility is that the superwind terminates when the rest envelope mass $M_{e,r}$ reaches a minimum value. Renzini (1981) suggests that this will occur when $M_{e,r} = 0.001$–$0.01\ M_\odot$. Using the expression for M_{lost} in Sect. IV, it can be shown that the maximum OH luminosity at the termination of the superwind is a function of the initial envelope mass $M_{e,0}$

$$L_{max} = \frac{M_{e,0}}{M_{e,r}}.$$

For $M_{e,r} = 0.01\ M_\odot$ we find approximately the same values for L_{max} as in Column 11 of Table 2. Both mechanisms effectively limit the OH lifetime and have a stronger effect on stars with low shell expansion velocities, due to their relatively lower envelope mass.

Substituting the above derived values for L_{max} in Eq. (12) and taking $L_s = 110$ Jy kpc^2, we get a corrected distribution $N'(M_{ms}, L_s)$ listed in Column 12 of Table 2 and shown in Fig. 4b. The fit is remarkably good, considering the uncertainties in the model and the fact that not all stars in the sample are located at the same distance. A lower sensitivity limit L_s, as is the case for surveys of nearby OH emitting Miras, will lead to the detection of relatively more stars with small v_e, since their lower maximum OH luminosity will also become detectable. Hence, the dependence of L_{max} on v_e or main sequence mass in Eq. (14) provides a natural explanation for the large differences Fig. 4a and b.

The introduction of a maximum OH luminosity as a function of v_e leads to a dependence of the OH luminosity distribution, $\psi(L_{OH})$, on v_e. For example, stars with $v_e = 11$ km s^{-1} (see Table 2) contribute to ψ as long as $L_{OH} < L_{max} = 112$ Jy kpc^2, and no longer for $L_{OH} > L_{max}$. The result may be a somewhat steeper OH luminosity function than the one we have used. Although this dependence of ψ on v_e is in contradiction with our earlier assumption that ψ is independent of v_e, this steeper slope is unlikely to significantly affect our conclusions.

Notice that the calculations are based purely on the observed circumstellar shell parameters, as derived from the OH observations. Only the stellar luminosity is derived otherwise, using the theoretical core mass-luminosity relation by Paczyński (1970). All calculations are based on a minimum OH luminosity of 1 Jy kpc^2, which is independent of v_e. However, the results turn out to be virtually independent of the exact choice of L_{min} within a range of 0.1–10 Jy kpc^2. The most critical parameter in the v_e-distribution is the slope of the IMF.

6. Synthesis of results and discussion

The statistical properties of OH/IR stars and their OH emission characteristics allow us to study the evolution of mass loss for low and intermediate mass stars on the AGB. The physical parameters of OH/IR stars indicate that they are at the top of the AGB and many of them are in the process of ejecting a dense circumstellar shell that may soon form a planetary nebula. They can therefore be considered as the end point of evolution on the asymptotic giant branch. The following evolutionary picture emerges. Initially an oxygen rich star on the AGB will enter the Mira instability strip with a relatively low mass loss rate (10^{-8}–$10^{-7}\ M_\odot$ yr^{-1}). This Reimers wind accelerates very slowly until it becomes sufficiently strong (1–4 $10^{-6}\ M_\odot$ yr^{-1}) for a saturated 1612 MHz OH maser to operate in the outer regions of the circumstellar shell. The maser will saturate when L_{OH} is approximately 1 Jy kpc^2. During the OH maser phase the mass loss rate is inversely proportional to the mass of the stellar envelope. It will accelerate as the envelope mass is reduced by the mass loss process until, during the last few percent of the OH lifetime, it increases approximately exponentially by more than an order of magnitude in a few thousand years or less, with a corresponding increase in L_{OH} of two orders of magnitude (see Fig. 3). The dense circumstellar shell will now totally obscure the embedded star. This is the phase of the strongest OH/IR stars.

The observations show that the OH luminosity depends on the size of the circumstellar shell and L_{OH} is found to be correlated with $\dot{M}$. This relation is consistent with the mass loss rates, derived

© European Southern Observatory • Provided by the NASA Astrophysics Data System

1983A&A...127...73B

independently from infrared observations. Assuming that the OH luminosity function for OH/IR stars reflects the evolution in time of L_{OH}, we find a quantitative relation for the evolution of the mass loss rate on the AGB, which includes a "superwind" phase near the end, when the star sheds most of its envelope mass in a relatively short time (1000–10,000 yr). The resulting dense circumstellar shell may be considered the planetary nebula precursor. Using the observed distribution of shell expansion velocities, v_e, for OH/IR stars we derive a relation between main sequence mass and v_e, which is in good agreement with the results of BHMW, based on the kinematics of these stars. This allows us to calculate at any point in the evolution of an OH/IR star its mass loss rate, rest mass, L_{OH} and R_{OH}. Alternatively, for an OH/IR star its present stellar parameters and the main sequence mass can be deduced from the OH emission profile and distance or shell size at which the maser operates (cf. Sect. 5 and the appendix).

The results of such calculations for a range of stellar masses at the beginning of the OH maser phase ($t=0$) are summarized in Table 2. They may be compared with those of Weidemann (1977) and Koester and Weidemann (1980), who studied the relation between the main-sequence mass and the final white dwarf mass using a large sample of observed white dwarf masses. In the picture developed in this paper the core mass at the beginning of the maser period is the final core mass of the evolution. We can thus equate $M_{co,0}$ (Column 4) with the mass of the central star of the planetary nebula and the mass of the white dwarf that will be the end product. Koester and Weidemann (1980) recommended two different relations ("FPR, $\eta=1$" and "BV–Wd non-linear" in their terminology); the second we have shown here in Column 6 indicated by KWII. The agreement with our results is close enough to be encouraging. A second comparison is with the pulsational stability analysis of LPV stars by Fox and Wood (1982). Comparing our M and $M_{co,0}$ with the properties they list, e.g. in their Table 2, it appears that our values of $M_{co,0}$ correspond to that time point in the stellar evolution when the growth rate in the fundamental oscillation mode starts to exceed that in the first harmonic mode. This supports the notion that it is the switch from first harmonic mode pulsations to fundamental mode pulsations that leads to the increase in mass loss (see also Wood, 1982). Finally we notice that the core masses for the onset of thermal pulsation by Iben (1981), given in Column 5 of Table 2, are between 10 and 30 % smaller than our core masses $M_{co,0}$, but follow the same trend.

The calculations by Fox and Wood (1982) lead to another interesting comparison. We have seen that during the OH maser phase the star loses mass at such a rapid rate that the core mass will not grow significantly and thus the stellar luminosity remains approximately constant. But the envelope mass decreases drastically and hence the pulsational period will increase. For example, take a star of 1.5 $M_\odot$. At the beginning of the OH maser phase its core mass is 0.7 $M_\odot$, and its luminosity is 1.2 10^4 $L_\odot$. Using again Table 2 of Fox and Wood we obtain a pulsation period of about 600 d. After 0.86 t_{OH}, or 170,000 yr, its total mass has decreased to 1 $M_\odot$, and its pulsation period has gone up to about 700 d. After 0.98 t_{OH}, when the mass loss rate has increased dramatically (see Fig. 3), its total mass has become 0.8 $M_\odot$ and its pulsational period is now 930 d. This example shows that OH/IR stars with the longest periods will have the highest mass loss rates. Such an effect has been noted by Engels (1982, see his Fig. 15).

In the picture developed in this paper, OH/IR stars are the last stage of evolution before the formation of a planetary nebula. This does not necessarily mean that all precursors of planetary nebulae are OH/IR stars or OH emitting Mira variables. In fact, carbon stars are also known to form planetary nebulae and, yet, they cannot form an OH maser because of the relatively low oxygen abundance. It is not clear to us where carbon stars fit in the evolution on the AGB. They may be a completely different category with a parallel evolution or, more likely, they may evolve preferentially from low mass stars ($<1.5\,M_\odot$) similar to OH emitting Mira variables, while most OH/IR stars appear to originate from stars with larger main sequence masses.

The two most important general conclusions of this paper are the following:

(1) Through observations of OH/IR stars it is now possible for the first time to study with *radio astronomical* techniques an important but poorly understood stage in stellar evolution, namely the final evolution on the AGB and the transition to the planetary nebulae.

(2) From the observed parameters of the *circumstellar shell* of an OH/IR star and its OH emission, we can deduce a variety of physical parameters of the *star* itself.

We find that our model of the superwind or OH phase, as described in this paper, is internally consistent and that it agrees with recent insights about mass loss during the AGB phase. We realize that it is rather schematic and that at several points a more thorough physical basis is required. Notably a derivation from first principles is needed to justify the Modified Reimers equation. It is encouraging to us that while no such derivation exists for the normal Reimers equation, it has nevertheless proven to be extremely useful.

Finally, from our model several predictions may be made that can be verified observationally.

1. The range in stellar luminosities, derived from these calculations, is consistent, with the observed luminosities in the infrared by Jones et al. (1982b), who found values between 2 10^3 and 6 10^4 $L_\odot$. Since the core mass does not grow significantly during the OH phase our calculations predict an increase in stellar luminosity, averaged over the light curve, with increasing v_e. Quantitatively this is shown in Table 2, Columns 1 and 7. Here we find that L_* must be proportional to v_e^2. Such a relation has been suggested by Salpeter (1974) on the basis of mass loss driven by radiation pressure, which is thought to be the driving force for the mass loss in these cool stars.

2. We do *not* expect a clear correlation between L_* and L_{OH}. For a star of a given L_* there could be a large range of values, depending on the state of evolution. A weak correlation may be seen, due to the lower maximum OH luminosity of stars with smaller main sequence mass (see Table 2).

3. More sensitive OH searches for OH/IR stars should turn up a larger fraction of stars with $v_e<10$ km s^{-1} than have been found so far (Fig. 4), because these stars will have intrinsically weaker OH emission. Indeed, more sensitive OH observations by one of us (BB) led to the discovery of several new, weak OH/IR stars. Most of these have $v_e<10$ km s^{-1}, consistent with our prediction.

4. Large OH luminosities correspond to high mass loss rates. From our model a correlation between L_{OH} and the infrared colours is expected, such as seen by Nguyen-Q-Rieu et al. (1979).

5. Large OH luminosities and very red infrared colours occur during the final stages when the envelope mass has become rather small and tenuous; hence, the pulsation periods of these OH/IR stars should be large. Such an effect has been found by Engels (1982).

6. In our view, stars reach their maximum bolometric luminosity on the AGB (and during the red stage of their evolution) during the OH/IR phase. If L_* on the AGB is a function of

© European Southern Observatory • Provided by the NASA Astrophysics Data System

1983A&A...127...73B

metallicity, then we should expect notable differences between the luminosities of OH/IR stars in the disk and those at the galactic centre, where the metallicity in stars appears to be enhanced strongly (e.g. Mould, 1982).

7. From Table 2 we find that the core masses of stars above a certain maximum main sequence mass reach the Chandrasekhar limit of $1.4\,M_\odot$ and probably undergo a supernova explosion before the mass loss rate is sufficiently high for the OH maser to operate. Hence, these stars will never become OH/IR stars. From Eqs. (A1) and (13) we find that this maximum main sequence mass for OH/IR stars is $6.5\,M_\odot$ and that $v_e < 22$ km s^{-1}. Indeed, only very few OH/IR stars are known with $v_e > 22$ km s^{-1} (cf. BHMW); the most notable are the M supergiants NML Cyg ($v_e = 24$ km s^{-1}) and VY CMa (31 km s^{-1}), whose properties are in many ways different from those of the majority of OH/IR stars. They are probably pre-supernova objects.

8. The measured OH shell size is a lower limit to the actual shell size. During the OH maser phase of a few 10^5 yr, matter is streaming through the OH emitting region to larger radii. For instance, for a star with $v_e = 15$ km s^{-1} and $\dot{M} = 10^{-5}\,M_\odot$ yr^{-1} the density n_{H_2} at a radius of 0.3 pc is about 20 cm^{-3}. We expect OH/IR stars with the highest mass loss rates, i.e. those that have lost most of their envelope mass, to have very extended and tenuous shells of the order of 1 pc in size and with a mass of about $1\,M_\odot$. Interestingly, some planetary nebula have a very large and faint halo around the main nebula, which may be the remnant of the stellar wind, preceding the nebula ejection (e.g. Capriotti, 1977). In our picture, these halos would indeed be the result of mass loss during the initial (say) 90% of the OH maser phase, when the parent star is still visible as a cool giant.

Acknowledgements. We would like to thank J. Herman for providing data on variability of OH/IR stars prior to publication, and P. Goldreich, J. W. Pel, A. Renzini, and A. I. Sargent for a critical reading of an earlier version of the manuscript. BB gratefully acknowledges financial support by NSF grant AST 78–21037. The Space Research Department at the University of Groningen is sponsored through the Committee for Space Research of the Royal Academy of Sciences by the Ministry of Education and Science.

Appendix

Here we discuss the calculation of the stellar parameters in Table 2 and the procedure to derive γ and δ.

1. For each value of v_e, the minimum mass loss rate at the onset of the OH maser phase ($t = 0$) is derived from Eq. (4) by assuming that the minimum OH luminosity for a saturated maser is 1 Jy kpc^2:

$$\dot{M}_{\min} = -1.8\ 10^{-7} v_e\ (M_\odot\ \mathrm{yr}^{-1}). \qquad \text{(A1)}$$

2. A reasonable estimate of γ and δ, based on the very crude relation between v_e and M from BHMW, yields a first estimate of M for each value of v_e.

3. Assuming an effective temperature of 2500 K for all OH/IR stars at the end of the AGB and using the core mass-luminosity relation [Eq. (11)], the mass loss equation (10) and the above values of $\dot{M}_{\min}$ and M, we derive an expression for the core mass at $t = 0$

$$M_{co,0} = 3.3\ 10^{-2}\ (v_e 10^{\frac{v_e - \delta}{\gamma}})^{2/3} + 0.5\ (M_\odot). \qquad \text{(A2)}$$

4. The initial envelope mass at $t = 0$ is $M_{e,0} = M - M_{co,0}$.

5. The stellar luminosity $L_{*,0}$ is derived from the core mass-luminosity relation. This is assumed to be constant throughout the OH maser phase.

6. t_{OH} is calculated using Eq. (7).

7. The mass distribution (Eq. 12) can now be calculated, assuming $L_{\min}$ and $L_{\max}$ are 1 and 1000 Jy kpc^2, respectively. The result is compared with the observed distribution for $v_e > 15$ km s^{-1}. This gives an improved estimate for γ and δ. Go back to step 3 and repeat the calculations until the fit to the ΔV distribution is satisfactory.

8. Using $L_{\max}$ from Eq. (14) the corrected mass distribution N' is calculated with Eq. (12).

References

Baud, B.: 1978, Thesis, University of Leiden
Baud, B., Habing, H.J., Matthews, H.E., Winnberg, A.: 1979, *Astron. Astrophys. Suppl. Ser.* **36**, 193
Baud, B.: 1981, *Astrophys. J. Letters* **250**, L79
Baud, B., Habing, H.J., Matthews, H.E., Winnberg, A.: 1981, *Astron. Astrophys.* **95**, 156 (BHMW)
Booth, R.S., Kus, A.J., Norris, R.P., Porter, N.D.: 1981, *Nature* **290**, 382
Bowers, P.F., Kerr, F.J.: 1977, *Astron. Astrophys.* **57**, 115
Bowers, P.F.: 1978, *Astron. Astrophys.* **64**, 307
Bowers, P.F., Johnston, K.J., Spencer, J.H.: 1981, *Nature* **291**, 382
Capriotti, E.R.: 1977, IAU *Symp.* **76** on *Planetary Nebulae*, Reidel, Dordrecht, p. 263.
Elitzur, M., Goldreich, P., Scoville, N.: 1976, *Astrophys. J.* **205**, 384
Engels, D.: 1979, *Astron. Astrophys. Suppl. Ser.* **36**, 337
Engels, D.: 1982, PhD Thesis, Bonn
Fox, M.W., Wood, P.R.: 1982, *Astrophys. J.* **259**, 198
Gehrz, R.D., Woolf, N.J.: 1971, *Astrophys. J.* **165**, 285
Goldreich, P., Scoville, N.: 1976, *Astrophys. J.* **205**, 144
Harvey, P.M., Bechis, K.B., Wilson, W.J., Ball, J.A.: 1974, *Astrophys. J. Suppl.* **27**, 331
Herman, J., Habing, H.J.: 1981, Physical Processes in Red Giants, eds. I. Iben, Jr. and A. Renzini, Reidel, Dordrecht, p. 383
Huggins, P.J., Glassgold, A.E.: 1982 (preprint)
Hyland, A.R., Becklin, E.E., Frogel, J.A., Neugebauer, G.: 1972, *Astron. Astrophys.* **16**, 204
Hyland, A.R.: 1974, Galactic Radio Astronomy, eds. F. J. Kerr and S. C. Simonson III, Reidel, Dordrecht, p. 439
Iben, I., Jr.: 1981, Effects of Mass Loss on Stellar Evolution, eds. C. Chiosi and R. Stalio, Reidel, Dordrecht, p. 373
Iben, I., Jr., Renzini, A.R.: 1982 (preprint)
Jewell, P.R., Webber, J.C., Snyder, L.E.: 1980, *Astrophys. J. Letters* **242**, L29
Jones, T.J., Hyland, A.R., Caswell, J.L., Gatley, I.: 1982a, *Astrophys. J.* **253**, 208
Jones, T.J., Hyland, A.R., Gatley, I.: 1982b (preprint)
Koester, D., Weidemann, V.: 1980, *Astron. Astrophys.* **81**, 145
Lada, C.J., Reid, M.J.: 1978, *Astrophys. J.* **219**, 95
Miller, G.E., Scalo, J.M.: 1979, *Astrophys. J. Suppl. Ser.* **41**, 513
Mould, J.R.: 1982, *Ann. Rev. Astron. Astrophys.* **20**, 91
Nguyen-Q-Rieu, Laury-Micoulaut, C., Winnberg, A., Schultz, G.V.: 1979, *Astron. Astrophys.* **75**, 351
Olnon, F.M., Winnberg, A., Matthews, H.E., Schultz, G.V.: 1980, *Astron. Astrophys. Suppl. Ser.* **42**, 119
Paczyński, B.: 1970, *Acta Astron.* **20**, 47
Reimers, D.: 1975, *Mém. Soc. Roy. Sci. Liège* 6^e Ser. **8**, 369

© European Southern Observatory • Provided by the NASA Astrophysics Data System

1983A&A...127...73B

Renzini, A.: 1981, Physical Processes in Red Giants, eds. I. Iben, Jr. and A. Renzini, Reidel, Dordrecht, p. 431
Rowan Robinson, M.: 1982, Monthly Notices Roy. Astron. Soc. **201**, 281
Salpeter, E.E.: 1974, *Astrophys. J.* **193**, 585
Schultz, G.V., Sherwood, W.A., Winnberg, A.: 1978, *Astron. Astrophys.* **63**, L5
Weidemann, V.: 1977, *Astron. Astrophys.* **59**, 411
Werner, M.W., Beckwith, S., Gatley, I., Sellgren, K., Berriman, G.: 1980, *Astrophys. J.* **239**, 540
Wilson, W.J., Barrett, A.H.: 1972, *Astron. Astrophys.* **17**, 385
Wood, P.R., Cahn, J.H.: 1977, *Astrophys. J.* **211**, 499
Wood, P.R.: 1982, contribution to IAU *Symp.* **103** on Planetary Nebulae

© European Southern Observatory • Provided by the NASA Astrophysics Data System